Bridging the gap between academia and operations for orbital debris risk mitigation

Mark A. Vincent
Raytheon

ABSTRACT

The operators of Earth satellites face a complicated process for making risk assessment decisions from orbital debris conjunctions. Some of these complications involve relatively simple parameters such as the hard body radius to use and thresholds of acceptable risk. Others are more complex, such as the proper predicted covariance of the two bodies and the desire to have confidence in how much the future probabilities of collision (Pc) might change. This paper explains all these issues and compares them to the academic work that has been performed. Although a gap is evident, some tools have been developed which can potentially aid the operators. The derivation of a new Pc forecasting tool, albeit similar to other tools, is presented. However, caveats for using all these tools are given, plus other examples where practical situations do not seem to match the theory presented in the literature.

1. INTRODUCTION

The Constellation Flying discussed in this paper refers to the process followed by the A-Train Constellation. It includes the following routine maneuvers. Drag Make-Up (DMU) maneuvers are used to keep the satellite in its control box, as shown by the vertical arrow in Fig. 1 representing an increase in semi-major axis. The control box is centered on its corresponding "virtual satellite" [1]. The real spacecraft remaining in its control box not only maintains its groundtrack close to its reference groundtrack [2] but also ensures that it will not cross the buffer zone and enter another constellation member's control box. The frequency of doing DMU maneuvers is a function of the control box size and the atmospheric density encountered but for the A-Train they occur typically every 4 to 6 weeks. Small orbit lowers are used by some of the constellation members to either prevent going out the back of the control box (due to an over prediction of the future atmospheric drag at the time of the DMU maneuver) or if trying to keep their groundtracks close to another satellite.

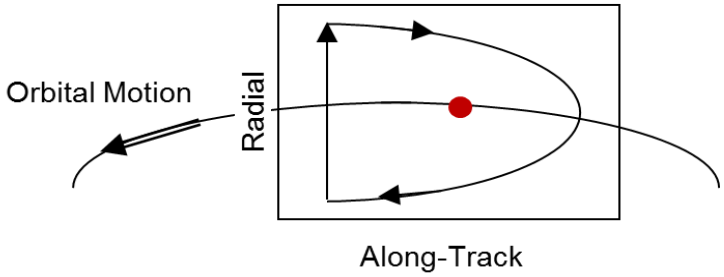

Fig. 1. Circulation Orbit within a Control Box

The A-Train also does coordinated annual Inclination Adjust Maneuvers (IAM) to counteract the luni-solar perturbation that increases the orbit inclination of all the members and thus keep their Mean Local Time of Ascending Nodes (MLTANs) within the desired range and close to being fixed with respect to each other [1]. Also note that the argument of latitude where the DMU are performed can be adjusted so that all the members keep their eccentricity vectors near the frozen value, as mutually agreed upon by the Mission Operations Working Group.

In this context of doing all these maintenance maneuvers, the onslaught of orbital debris has had a profound effect. So much so, that during most of the year (except perhaps during the IAM campaign) monitoring conjunctions and designing and implementing Risk Mitigation Maneuvers (RMMs) takes up the majority of the satellite operators' time. The following sections discuss specific issues, processes that have been developed, and potential flaws in these processes. Academic investigations are compared to practical situations and where disagreements are apparent, future analysis is suggested.

2. OPERATIONAL ISSUES

Staying within the Box

Staying within the control box adds an extra complexity to designing RMMs. First it should be noted that half the satellites in the A-Train do not have the capability/desire to do orbit lowering maneuvers, at least not until they do the retrograde maneuvers to exit the Constellation at the end of their missions. Therefore all their RMMs are orbit raises. Currently the GCOM-W1 satellite is spending many months outside the back of its control box because it had to do multiple (orbit raising) RMMs. Luckily there was plenty of extra buffer between it and the Aqua satellite behind it and it will be returning to its control box sometime this fall.

Aqua itself does not do orbit lowering maneuvers; however, it has had only short excursions outside of its box. But this is partly due to intensive trades between doing RMMs that safely mitigate the threat of conjunctions and not doing the maneuvers so large that they push it out the back of the box. A lesson learned in all this is that for constellation flying, it is highly recommended that satellites either have the capability to turn around 180 degrees from their orbit raise orientation to do orbit lowers, or if their instruments (or sensors) do not permit this (as the case for Aqua and GCOM-W1) then to have thrusters mounted in the appropriate places to do the orbit lowers without these large slews.

Even having the capability to do orbit lowers does not help when approaching the front of the control box with an impending DMU (though often an early DMU is used to alleviate a future conjunction). That is, either the orbit lower has to be immediately followed by a (larger) DMU or the spacecraft will come out of the front of the box. Plus, as described in the Timing subsection, about half the time there is a preferred choice between an orbit raise or lower, where "preferred" implies mitigating the risk with a much smaller RMM.

Choosing a Hard Body Radius

The combined Hard Body Radius (HBR) is an important parameter in risk mitigation because the Probability of Collision (Pc) is approximately equal to the square of the combined HBR. It is a linear combination of the HBRs of the primary and secondary objects. One conservative method defines the HBR to be the radius of a sphere that is centered on the center of mass of the body and contains the whole body. Or alternatively this can be thought of as a radius of a circle centered at the center of mass that contains the body in any orientation. The applicability of the 3-D vs. 2-D model is discussed more in the Pc calculation subsection. The reason both models are quite conservative is the fact that the body is usually not spherically symmetric about the center of mass. An extreme example is the Aqua spacecraft which has just one large solar array which is attached by the short side to the side of the bus (Fig. 2a); the Orbiting Carbon Observatory II (OCO-2) is not quite so conservative, with two solar arrays attached on their short ends (Fig. 2b) and finally, CloudSat with two arrays attached by their long sides (Fig. 2c) is the least conservative, though it still has some margin.

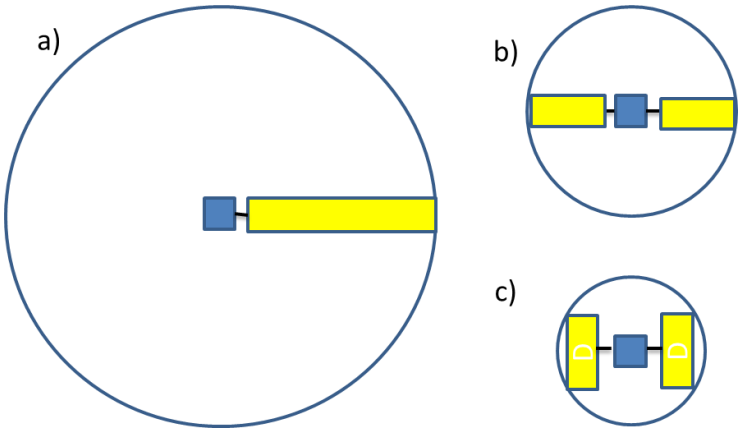

Fig. 2. HBR Examples

The margin involved can be thought of the volume/area of the sphere/circle not "filled" by the observatory. Using the "center of figure" rather than the center of mass introduces a small error since it is the trajectory of the center of mass that is solved for in the orbit determination process, though this error can be thought of as just a shift in the (bivariate) probability distribution function and is less of an issue near the tails of the distribution.

In all cases there is a minimal value for the HBR. This minimal value or slightly larger (for some margin) is chosen for the Primary object. For the Secondary objects there is a distribution of sizes, namely from the smallest objects that can be tracked to large intact rocket bodies or spacecraft. NASA's Conjunction Assessment Risk Analysis (CARA) has recommended a practical choice of 1.5 m which represents the 95th percentile of catalogued objects in LEO orbit [3]. This choice is confirmed by data provided earlier by the CloudSat mission that indicates 1.5 m as the 94.1th percentile value [4]. The caveat being that, if a secondary with a known larger HBR, such as rocket body, is producing a conjunction in the future, then that the combined HBR can be increased accordingly for analysis done during the time period leading up to the decision whether to do the RMM.

Choosing Pc Thresholds

There are several Pc thresholds of interest, though the most important is the value that is used to determine if a RMM should be performed, at the time that decision is made. The commonly used value for this is $1x10^{-4}$. A heuristic approach to arrive at this value is to start with a NASA requirement that the total risk over the active mission from orbital debris should not be more than $1x10^{-3}$. The binomial expansion gives the total probability P_T from n events, where the probability from a single (collision) event is P_i, to have leading terms:

$$P_T = 1 - (1 - P_i)*n + \ldots = n*P_i + \ldots$$

This "cumulative probability" is sometimes controversial, so it is important to understand what it represents. Assume Pi is the threshold and consider events that having a probability $P_i - \varepsilon$ where ε is an infinitesimally small number. Thus for n = 10 then the P_T is approximately $1x10^{-3}$ for a $P_i = 1x10^{-4}$. Again, the value n=10 is chosen somewhat arbitrarily, and to do this rigorously all the events with probability less than P_i would have to be summed up. But the salient point is that all these risks below the threshold are accepted, specifically no RMM is performed. So the choice of $1x10^{-4}$ for the threshold is assumed to cover this cumulative effect, with extra margin added from a conservative choice for HBR.

One of the auxiliary thresholds of interest is the value used to determine when to start planning the RMM. So with all this in mind, using a threshold with $1x10^{-5}$ is a reasonable choice to start the RMM planning. Note there is one caveat to this, if the secondary is an active satellite then it should be confirmed at a lower threshold ($1x10^{-7}$) that they are not going to maneuver before the Time of Closest Approach (TCA), if possible.

Another threshold of interest is the acceptable post-maneuver Pc from any object. The complicating factor here is that currently the maneuver execution error is not included in the calculation of these Pc's. This subject is discussed more below. So until this uncertainty is implemented properly, some suggested values from the OCO-2 mission are: that it is desirable that the Pc with the original object or any new objects be less than $1x10^{-6}$, however under extenuating circumstances, less than $1x10^{-5}$ would be acceptable. However, these scenarios have led to a new discussion and tools being built for multiple secondaries. The general consensus is to reduce the overall risk; however just as is the case for a single secondary, timing and operational considerations are important. This is further discussed in the Risk Determination and RMMs subsection.

Attempts been made to add more of a statistical basis for the decision-making process. The Wald Sequential Probability Ratio Test [5] includes miss detection and false alarm criteria. Although this is a good example of bridging the gap between theory and practice, it does raise new questions. For example, how large of a miss detection threshold (i.e. when a collision is going to occur but the no detection/action occurs) is really acceptable? One argument would be that the probability for any given satellite having a collision is small so a small probability of missing it is okay, however this argument tends to break down if considering multiple satellites each several potential collisions over their lifetimes. It is also adding an uncertainty to an uncertainty similar to the Pc forecasting tools discussed later in this paper.

Timing is everything

Conjunctions with secondary objects can be predicted as early as a week before TCA. However the correlation between the Pc's at this time is low compared to later values; in fact CARA now doesn't report conjunctions until TCA – 5.5 days [6]. During the time period between TCA - 5.5 days and TCA – 2.5 days, conjunctions can be monitored and planning of RMM, if prudent, is started. The time period between TCA-60 hours and TCA-12 hours is crucial for the final designs, approval and upload of the RMM if it is necessary. Note these time segments are representative and vary by mission, though the underlying probability is the same (albeit still a function of HBR).

One of the factors involved in the timing is the RMM method used to mitigate the risk. One choice is to use a small RMM earlier on (that is, a longer time before TCA) so that the small orbit raise or lower causes an accumulated alongtrack separation. The other choice is to perform a larger RMM on the opposite side of the orbit from the location of the closest approach that utilizes the radial separation to mitigate the risk of the conjunction. That is, the latter implies doing the RMM 0.5 or 1.5 or… orbits before the TCA.

Perhaps the most important factor is the relationship between the miss distance and the uncertainty of the states of the two bodies that creates a time-dependent Pc with respect to the TCA. The natural tendency is for the uncertainty to decrease as TCA approaches, mainly due to the reduced time period of the orbit/covariance propagation between new orbit determinations and the conjunction. Thus the Pc first increases to a maximum value and then rapidly decreases, assuming that a collision is not actually occurring! This can cause operational difficulties since the maximum can occur near the comfortable time to make the decision on the RMM, for example 48to 36 hours before TCA.

Fig 3. is similar to ones presented in a landmark paper by Alfano [7]. For plotting purposes a spherical covariance assumption is made. Specifically this means that the two vectors in the conjunction plane ("b-plane") perpendicular to the relative velocity, one in the direction of the Miss Distance and the other perpendicular to it, have the same (position) covariance. When there is a long time to propagate from the last observation to the TCA this uncertainty at TCA is high. As shown on the left-hand side of the figure, this implies the Pc is relatively low. This situation has sparked a lot of debate in the conjunction community and perhaps should be called the "conjunction paradox" or implying that "ignorance is bliss." Specifically it means if no other measurements are taken and the maneuver threshold has not been exceeded then theoretically no action should be taken (and *vice versa*). However, the way to unravel the paradox is to realize that current measurement is only an estimate of the underlying Pc. Therefore it is not only prudent to take as many more measurements as possible, it is mandatory to fulfill the real intention of mitigating the risk of a conjunction.

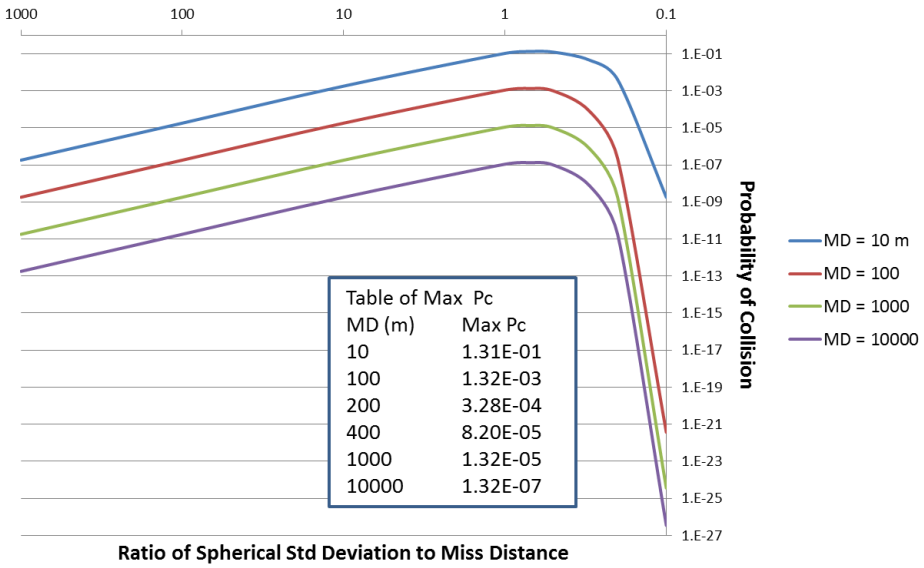

Fig. 3. Generic Pc Behavior for a HBR = 6.0 m

As the time to TCA decreases and the uncertainty in the miss distances decreases, for a given Miss Distance the Pc increases to a maximum value. The ratio that produces this maximum Pc is 1/sqrt(2) as previously published in [7] and is inherent in the Pc Calculation subsection below. As the ratio continues to decrease, the Pc drops off rapidly, assuming that the situation is not of an actual collision. The biggest caveat in interpreting this plot is to remember that for each update to the conjunction, not only does the covariance change (note if there is no new tracking there will only be a small decrease in the covariance from updated solar flux and other similar parameters) but the Miss Distance, in general will also change, in other words, a jumping of curves on the figure. However there is a probability distribution involved in how much the Miss Distance changes; this will be discussed further in the Tools and Future Plans section.

Designing an RMM

Choosing the magnitude, and as was discussed earlier, the direction, of an RMM depends on the geometry involved, the desired post-maneuver Pc and other factors such as control box position. If the cross-track and alongtrack components are rotated into a single vertical plane so that the secondary is either ahead or behind the primary (i.e. crosses the primary orbit plane before or after TCA). Then the geometry can be divided into four quadrants as shown in Fig 4.

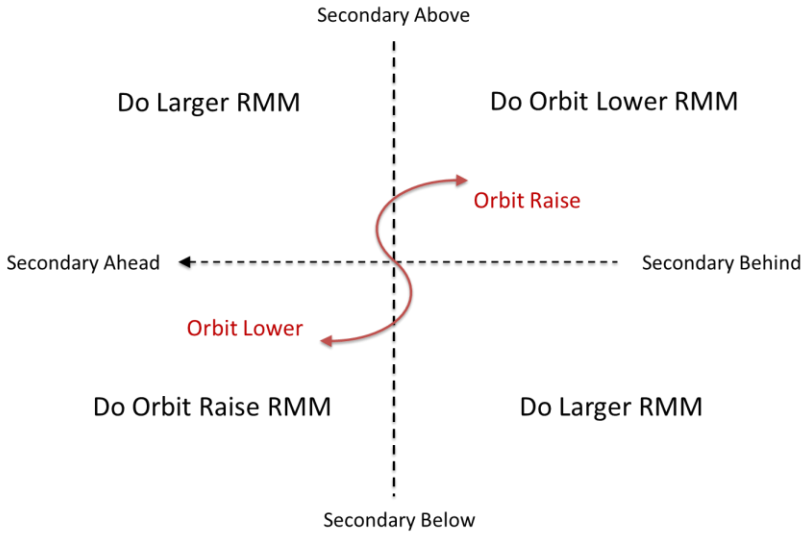

Fig. 4. Simple RMM Choices

If the secondary is in two of the quadrants the preferred RMM direction is obvious. Specifically, if the secondary is in front and below the primary then an orbit raise by the primary not only increases the radial separation but also after the first about third of an orbit, it will also increase its cross/alongtrack separation. The opposite is true for a secondary which is behind and above the primary, thus an orbit lower is chosen. The other two cases are more complicated since the radial and cross/alongtrack effects "counter benefit" each other. In these cases all the parameters have to be weighed carefully and in general a larger RMM is required. For example, if initially the radial miss distance was a small positive value (i.e. secondary slight above) and the secondary was ahead, a larger orbit raise would put the primary above and well behind the secondary. CARA calls this "burning through the conjunction."

3. RELATED RESEARCH

Consider five phases of the conjunction risk mitigation: Tracking, Orbit Determination, Orbit/Covariance Propagation, Risk Determination and possible RMM design and implementation. Lumping the first two together and similarly the last two, the following provides a brief summary of the research efforts.

Tracking and Orbit Determination

Rather than try to cover the vast subject of different tracking methods and orbit determination techniques, some of the aspects relevant to operational issues will be focused on. Obtaining the observations used to create a definitive ephemeris is discussed first, while the propagation of those ephemerides constitutes the next subsection. Methods to track (larger) active satellites include GPS and other range and range-rate radiometric observations and satellite laser ranging. There is some uncertainty in these definitive ephemerides but it is relatively small and contributes to a lesser degree in the prediction uncertainty than the contribution from atmospheric drag uncertainty. The retroactive comparison of deterministic values to what had been predicted for them is discussed more in the next subsection. The tracking of orbital debris and (smaller) satellites without their own tracking capabilities is done by radar or optical measurements from the ground. This introduces new issues such as sparse observations, implying both a long time between observations and the possibility of a single observation during a pass plus the issue of object identification (or misidentification). Overall this creates a larger uncertainty in their definitive ephemeris and the uncertainty propagated to TCA that is relevant to the conjunction process. It is worth noting that the present lower limit of the size of the objects that can be tracked reliably is about 10 cm. In the future, this value will be reduced significantly. Ostensibly this will "improve" the situation of avoiding orbital collisions but a lot of the operational issues presented in this paper will be greatly exacerbated when there is an order of magnitude or more new objects to be concerned with.

Orbit/Covariance Propagation

Orbit state and covariance propagation are part of the orbit determination process. This subsection will address how their definitive solutions are propagated into the future to do conjunction risk assessments. However, some of the issues with propagating into the future are inherent in the orbit determination process, as indicated by the large number of filter choices in Fig 5. A large volume of academic research has concentrated on the issue of how best to propagate the covariance associated with satellite state values into the future. The two main issues that are addressed are a) whether the non-linear dynamics involved in the state propagation can be linearized (see Fig. 5) and still produce good results, and b) whether the model of the non-linear forces is adequate in the first place. There is also a discriminator related to there being a linear of non-linear relationship between the observables and state parameters.

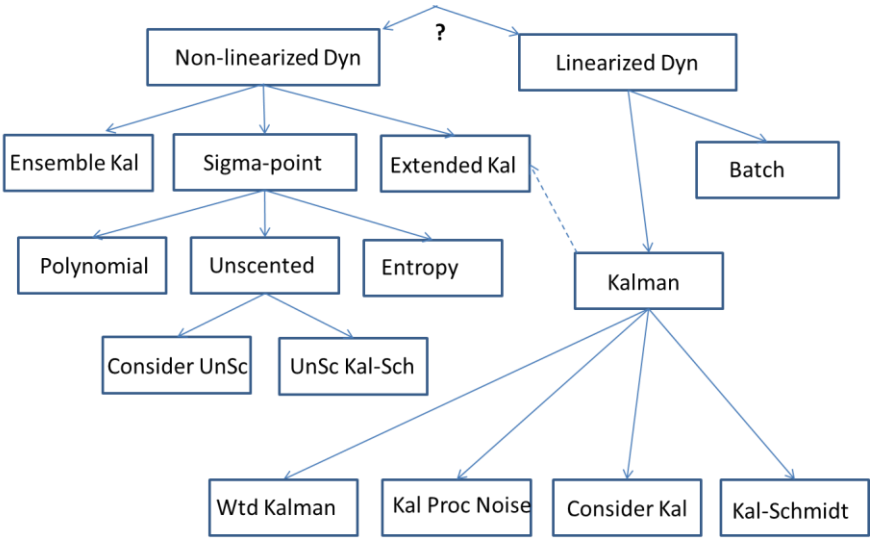

Fig. 5. Filter Choices

One of the aspects of the linearization is the orbit element set that is used. The standard example of non-linearity growing to significant levels is the integration of Cartesian elements over an extended time period. However, as described above, when the number of days to TCA is 4 or 5 days or longer the emphasis is to wait for more observations anyway. However, using Keplerian, Poincare or Equinoctial elements consisting of five slowly

changing elements and one fast-changing element, make the non-linearity even less of an issue. Theoretical studies have determined the limits to which the covariance manifold can be reduced from the choice of variables [8, 9].

If linearization of the dynamics is appropriate, there is a great advantage that the covariance can be propagated with the same state transition matrix used to propagate the state elements. Without linearization the covariance matrix elements must be integrated with the full force model. If this is done in a full-factorial or Monte Carlo method, the computational time can be a burden, if not prohibitive. Thus the concept of "sigma-points" was introduced so that just a subset of the representative points of a covariance manifold need to be propagated. The most famous of these methods is the Unscented Kalman Filter [10]. Newer methods use polynomials [11, 12] or entropy values [13] or mixed models [14]. A good comparison of sigma-point Kalman filters vs. Extended and Ensemble Kalman filters is given by Ambadan and Tang [15]. They point out that the Extended version still relies on linear assumptions for propagation (hence the dashed arrow in Fig. 5) and the Ensemble version still has the linear observation/state relationship (though if the non-linear case the solution can be iterated). Also, since it is essentially a Monte Carlo technique, a large number of state variables and/or ensembles can lead to computational burdens.

The modeling of forces is a more complicated issue. To pick the dominant example, predicting the future solar activity and resulting atmospheric drag has been investigated by many parties and the models are often updated. However, it is important to note that usually risk determination methods include the predicted solar activity models in the state propagation but not the covariance propagation, an exception being the covariance supplied to CARA by the Joint Space Operations Center (JSpOC), as described below.

Several methods have been developed to account for the fact that the covariance propagation does not include all the relevant force modeling. One is to include consider parameters which are not estimated, but whose uncertainties are included in the covariance, see Chapter 6 of [16]. A good comparison of using consider parameters versus other Kalman Filter enhancements, in particular the Schmidt method, is given by Stauch and Jah [17]. The mis-modeling of the drag parameters is accounted for by the JSpOC by increasing the corresponding covariance terms. Presently a fixed value is used for this consider term, but future enhancements will include dynamic (i.e. fitted) consider parameters for both the uncertainty of the future solar flux and the ballistic coefficient of the spacecraft [18].

Another method used to adjust the covariance (usually to increase it) is to include "process noise," see p. 220 of [16]. This can be thought of as scaling the covariance, either in a uniform manner or for selected terms. One method is to compare to past deterministic covariances [19]. Scaling is a bit of an art and methods are available to determine if the values used are appropriate [20].

Another uncertainty due to a "force" that is of great interest is the maneuver execution error. Most of the current Pc calculation processes do not include it, however research is being done [21] and it is a priority to include it. A note of caution, most spacecraft manufacturers are very conservative in their advertisements of the capabilities of their propulsion systems. However, adding a lot of extra uncertainty is not necessarily good for the risk mitigation process. If one is on the left-hand side of Fig 3. this uncertainty can suppress a Pc and void when an RMM actually should have been performed. Likewise if one is on the right-hand side the extra uncertainty can inflate the Pc and cause an RMM to be performed when it actually was not needed. That is why fitting parameters to past performance to determine the maneuver uncertainty is a possibility [21]. One caveat to the maneuver execution error issue is that the immediate change in the orbit is small, it is the alongtrack error build up that becomes significant and the problem is bounded on the other side after the first post-maneuver tracking is obtained. So for reasonably small maneuvers one can think of the 6 to 24 hour time period after a maneuver as a typical period of concern for the effect of this added uncertainty.

Risk Determination and RMMs

One of the latest areas of interest is calculating the overall Pc from multiple secondaries for different maneuver options (including no maneuver) [22]. This scenario will become even more relevant when the number of tracked objects increases. However, the issue of timing becomes more complicated. For example, a conjunction just below the threshold with a TCA two days away may combine with a medium risk with a TCA four days away for a total Pc greater than the threshold even though accepting the first conjunction and the risk from the second one disappearing is a possibility. Even less desirable, performing an RMM to mitigate the first conjunction might make the second one worse and force a second RMM. Differentiating between these options will be difficult and might benefit from

some sort of Pc prediction (see next section) to account for an observation between the first and second conjunction. Another possible enhancement would be to make a "Pareto efficient" option, that is, only consider maneuvers that do not make the Pc from *any* particular conjunction worse than it is from doing no maneuver.

4. TOOLS AND FUTURE PLANS

Pc Calculation

The calculation of the Pc for objects moving past each other at a relatively high rate, the so called 2-D solution is reasonably straightforward. There are several implementation methods that can be compared for accuracy and speed of calculation [23]. Below is the description of a method that has been implemented into a spreadsheet. For objects moving past each other at a relatively low speed, the so-called 3-D solution has also been published [24, 25] and will not be discussed here.

The first step in the 2-D solution is to combine the position uncertainties of the two objects by adding them in a common coordinate system. This combined covariance is then rotated to find its components in the "conjunction plane" (similar to the b-plane used for interplanetary targeting). This plane is perpendicular to the relative velocity of the two bodies and desired components are with respect to a vector in the relative position direction (called the Miss Distance direction) and a vector perpendicular to it (here called the Perpendicular direction). These two covariances form a bivariate probability distribution as shown in Fig. 6. Here the origin represents the position of the primary object (of infinitesimal dimension) while a circular cross-section at x = MD (the miss distance) and y = 0 represents the secondary object with a circular having the radius equal to the combined HBR (note some methods have the primary and secondary switched). The probability of the primary actually being in the circle (a collision!) is the volume of the cylindrical tube with the aforementioned circular base area and a top conforming to the shape of the bivariate distribution. This is analogous to the area under the curve in the univariate distribution (such as shown in Fig. 7). Also note that for the spreadsheet analysis which was used for the results in this paper, rather than a circular cross-section, a square was used to facilitate the calculation of the tube volume. However, a scaling factor of $\pi/4$ must be used that is essentially making the area of a square base equal to that of the original circular one. This is a very good approximation for the small values involved. If NC is used to represent the normal cumulative univariate distribution with mean μ and standard deviation σ:

$$NC(z, \mu, \sigma) = 1/(\text{sqrt}(2\pi)*\sigma) * \exp[(z-\mu)^2/2\sigma^2)]$$

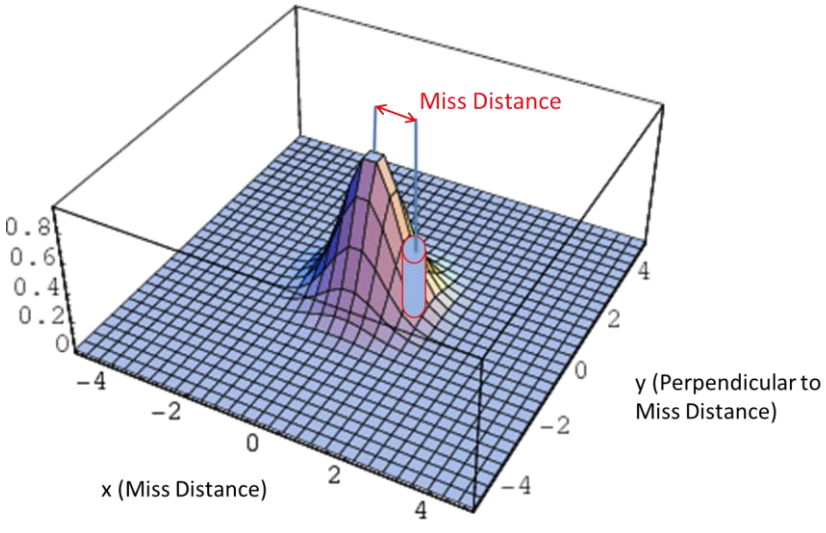

Fig. 6. Pc Calculation from a Bivariate Distribution

Then the volume of the tube is simply:

$$[NC(MD+HBR,0,\sigma_x) - NC(MD-HBR,0,\sigma_x)] * [NC(HBR,0,\sigma_y) - NC(-HBR,0,\sigma_y)]*\pi/4$$

where x and y are the coordinates shown in Fig. 6 and σ_x and σ_y are the respective standard deviations.

Pc Prediction

As mentioned above, each new observation will produce (in general) a different miss distance. Operationally this translates to an apprehension that a future Pc will "suddenly" jump to a high value, requiring a rapid decision process and a possible RMM. Several papers have been published on this topic [26, 27, 28] The following describes my tool which is similar to Duncan's [26] although the two were developed independently. In particular, both determine a confidence level (that actually is a probability distribution) that a future Pc will exceed a given threshold after new tracking data is acquired. To explain my Pc Tool, start with the 1-D analogy shown in Fig. 7.

On the left-hand side is the standard depiction of the how the Pc in this univariate example is the area under the curve centered at the MD calculated at t_0, representing the probability that the primary object is not at the origin, but rather in the shaded area. The blue curve has zero mean and a standard deviation σ_0.The right-hand side depicts the situation at t_1 in which the original coordinate system of the primary is now a distance Δ towards the secondary creating a new coordinate system in which the red curve represents the new probability (of where the primary actual is), again with zero mean but now a new standard deviation (σ_1) representing the uncertainty after a new observation is taken at t_1. Plus a new miss distance, MD_1 which is simply $MD_0 - \Delta$. Up to this point this description has been (hopefully) straightforward. However, the not so obvious contention is that the parameter Δ has the same probability distribution as MD_0. Keep in mind that at both time points the distribution is for the condition at TCA. So in colloquial terms the probability that MD_0 is actually MD_1 is dictated by the distribution of MD_0 *a priori* to the new observation and the new observation just makes MD_1 the estimate of the most likely miss distance with a new σ_1.

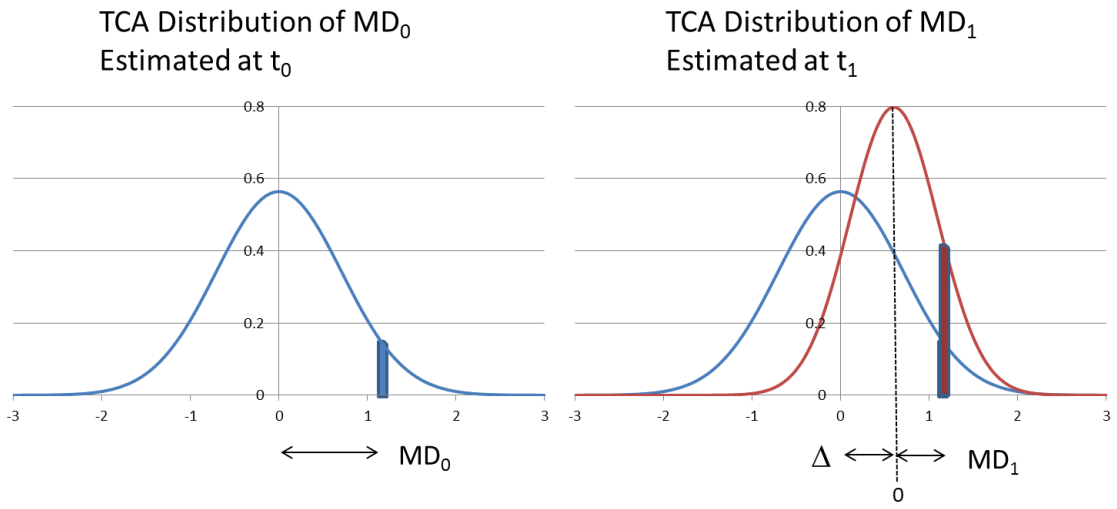

Fig. 7. Univariate Distribution a t_o and t_1

Before describing the algorithm for calculating the confidence in what Pc is at t_1 (Pc_1) it should be emphasized that the preceding describes the distribution of Δ (and hence MD_1), but predicting the value of σ_1 is a different matter. This will be discussed in the final part of this subsection. For now it will be treated as an input parameter to be varied so contour plots like Fig. 8 can be produced and discussed. The following describes how the tool was built in a spreadsheet, though a computer program could create the plots with higher precision and in a faster manner.

Remaining with the 1-D analogy in Fig. 7, the preceding discussion pertained to one realization of Δ/MD_1 and its corresponding Pc_1. As a side note, Pc_1 (area of red solid) was greater than Pc_0 (area of blue solid) because the reduction in the miss distance overwhelmed the fact that $\sigma_1 < \sigma_0$. If Δ had been negative (which had 50% chance)

then the same σ_1 would have produced a Pc_1 much less than Pc_0. In general, what the spreadsheet tool does is divide the MD_0 distribution into bins. As a very coarse example, consider the bins to be (values are in standard deviations):

$$(-\infty, -3), (-3, -2), (-2, -1), (-1, -0.5), (-0.5, 0), (0, 0.5), (0.5, 1), (1, 2), (2, 3) (3, +\infty)$$

Each bin will have an associated probability (of Δ falling into it), call it Q_i. Plus each bin's center point will have an associated Pc_i. Therefore, to create a confidence metric all the Q_i when Pc_i is less than the threshold will be added to give a total Q_T. This Q_T is the confidence that Pc_1 will not exceed the threshold. In the above simple example, say the leftmost 8 bins had Pc_i less than the threshold. The confidence that Pc_1 was not above the threshold would be 97.725% , that is the probability of being below 2-sigma for a standard deviation. This describes the 1-D example; the Pc Tool does it in two dimensions. The second dimension in this case was described in the Pc calculation as being perpendicular to the MD direction, so the analogy to MD_0 in this dimension is zero.

To create the plots such as Fig. 8, some choices have to be made to fix some of the multiple parameters of the problem. The first is to choose the first miss distance MD_0. Next, similar to Fig. 3, the spherical choice $\sigma_{x0} = \sigma_{y0} = \sigma_0$ and $\sigma_{x1} = \sigma_{y1} = \sigma_1$ are made so σ_0 and σ_1 can be used as the two axis on the contour plot with Q_T being the contour (color) value. Note the choices of making the standard deviations spherical is only for plotting purposes, the tool itself can produce a Q_T value even if all four σ's are different.

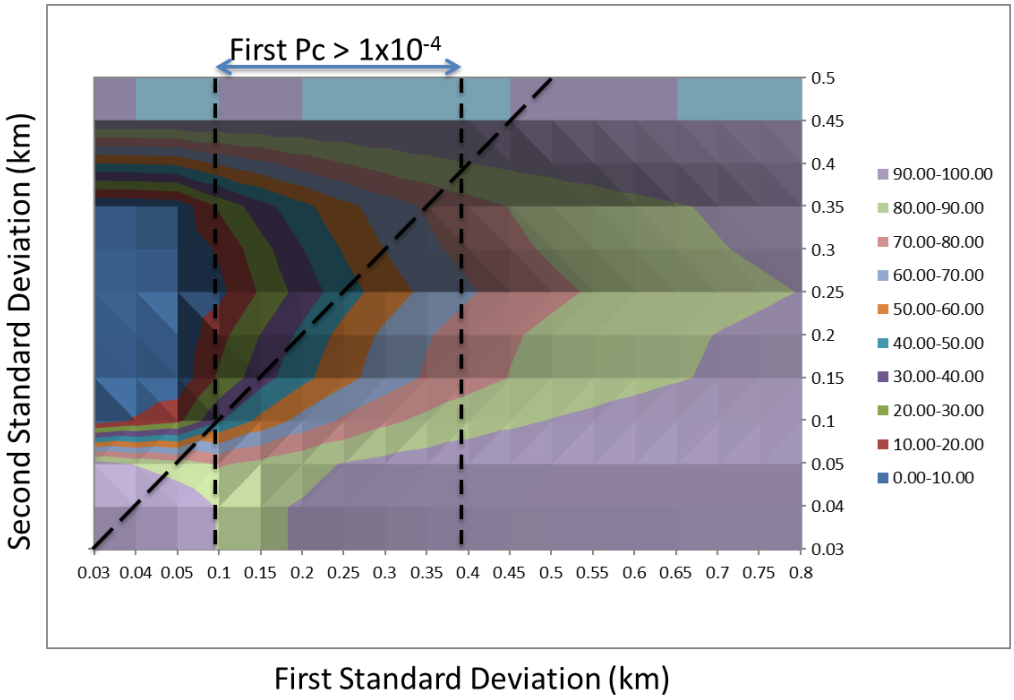

Fig. 8. Confidence in $Pc_2 < 1 \times 10^{-4}$ with $MD_0 = 200$ m and HBR = 6 m

The results in Fig. 8 warrant some discussion. The pixilation caused by finite bin size and the way that PowerPoint produces contour plots is evident especially at the top of the graph. Smaller bin sizes combined with more automation will allow for better precision and faster plot generation. The diagonal dashed line is simply when $\sigma_1 = \sigma_2$, so for practical reasons it is better to focus on the area below the line when $\sigma_2 < \sigma_1$. That is assuming the new observation decreases the uncertainty at TCA. The region between the vertical lines is also interesting since it represents the converse problem that discussed above. In this case Pc_0 has already crossed the threshold and the confidence level represents the action that the new data will relieve the issue as Pc_1 falls below the threshold. The small region to the left of the vertical lines plus the region right of the lines represents the previously discussed case where Pc_0 was okay but there is concern that Pc_1 will cross the threshold. The general conclusion is that the confidence is quite high (70 to 100%) that this will not occur. The center left of the plot is where there is dynamic

variation in the confidence level and (with $\sigma_1 < s_0$) the confidence drops down in the 30% range. An important fact in this area is realizing that for a MD = 200 m, the maximum Pc is when $\sigma_0 = \sigma_1 = 141$ m (per Fig. 3).

As mentioned earlier there is the question of how to estimate σ_1. Simplifying the problem greatly to single measurements propagated to TCA, then if the uncertainty is increasing quadratically and t_0 is 4 days to TCA and t_1 is 2 days to TCA then $\sigma_1 = \sigma_0/4$. One of the complications to this model is the fact that there are multiple observations over a fit span used in the orbit determination. This is actually a sensitive factor in calculating Pc in general, in particular what fit span to use and how to de-weight older observations. For example, if a weekly fit span from TCA-11 days to TCA-4 days is updated on TCA-3 days creating a new fit span from TCA-10 days to TCA-3 days, then how much the older measurements are de-weighted (if at all) in both solutions will influence how much the new observation will change Pc. Or an alternative question, if the Pc changes dramatically when comparing a fit over the past 7 days to the past 6 days, how much confidence is there in either calculation? In particular, for cases that have been seen in the past, where one or more of the RIC (Radial, In-track, Cross-track) components appears to be converging to one value during the early days but then takes a "multi-sigma" jump and starts converging to a different value. This is discussed further in the next subsection. And returning to the Fig. 8 discussion, the choice of fit span will influence what the estimate of σ_1 would be. Analyses of using the trends from the current conjunction [27] and both the current and past conjunctions [28] have been performed.

There is another fundamental issue with the implementation of the Pc Tool. That is, how does a confidence level affect operations? One factor to keep in mind is that the observation at t_1 will be taken anyway and if the conjunction still occurs within the appropriate volume, Pc_1 will be calculated. The practical answer appears to be that it will only be in the extreme ends of the confidence levels, say the 0 to 10% and 90 to 100% where any influence would happen. And more importantly, this influence might only be in the staffing and level of effort (for example, asking for more tracking or doing maneuver design) regimes. But hopefully discussions with mission operators and real-life examples can be used to determine if a Pc prediction tool is worth pursuing. One benefit that is hard to quantify would be the reduction of the stress level of the operators worrying that future Pc's will surprise them.

Counter-examples seen in Operations

The jumping of miss distances and Pc values, and the concern about it happening in the future is arguably the biggest concern of Operations. Fig. 9 represents two scenarios that have been seen in A-Train Operations although the data itself is fictitious.

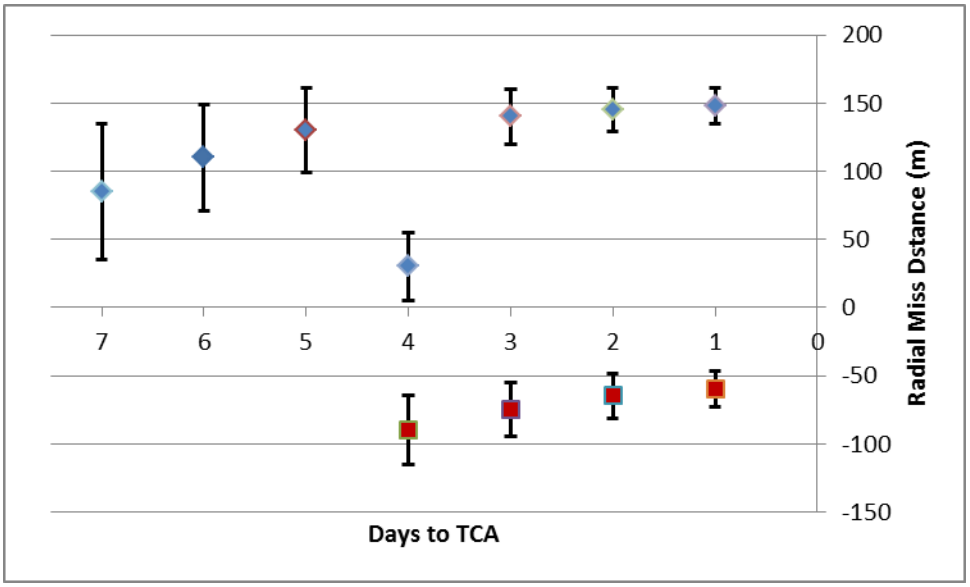

Fig. 8. Examples of how Miss Distances can Jump

In the both cases the trend of the predicted Radial Miss distance (RMD) at TCA is good from TCA-7d to TCA -5d. In the first scenario (all blue diamonds) the RMD drops down to a small value but by TCA-3d it went back up to a relatively safe value. Meanwhile the uncertainty indicated by the error bars has continued to decrease as the new observations (each day) are made. It is rather easy to dismiss the prediction on TCA-4d as just a bad solution from bad tracking. However there are a couple of issues with this conclusion. First, really bad tracking such as a pass with only one radar observation is usually discarded. And second, as described above, there is the question of why the new data was so heavily weighted causing the older tracks to have such a small influence on the solution at TCA-4d. There is also the possibility that the wrong object was tracked just before the TCA-4d prediction. Object recognition is an important part of the overall space situational awareness process, but it won't be discussed here.

In the other scenario, the solutions jump from the blue diamonds to the red squares on TCA-4d. This has caused some consternation (and preliminary RMM planning) from operators because it raises questions about the validity of the blue diamond solutions and whether the uncertainties shown for the red squares are valid. Or alternatively expressed: why was there a multi-sigma jump on TCA-4d? The most recent example of a case like this did have a two-day gap between the equivalent switch from blue to red tracks and a solar flare during that gap, however previous similar cases did not have these extenuating circumstances. Overall, more analysis of the tracking and orbit/covariance determination processes is definitely warranted to try and avoid future occurrences of these situations.

5. CONCLUSIONS

The bridge between academia and operations for conjunction risk assessment is a work in progress. Although a number of sophisticated theories have developed, especially for covariance propagation, they have only been implemented to a limited degree, especially in the decision making process. And even when the algorithms have been implemented (for example, in the case of process noise) there remains the need to tune the parameters, which opens up new opportunities to add rigor. Plus the goal remains to add more physical models rather than relying on more heuristic techniques. But adding more force models creates more parameters to be estimated or considered and compounds the curse of dimensionality [13]. Nevertheless, having the confidence that calculated Pc represents the actual risk to the best extent possible makes the decision process easier, including the adherence to firm maneuver thresholds.

6. ACKNOWLEDGEMENTS

The author would like to thank Dr. David Baker for his review of this paper and the OCO-2 project of the Jet Propulsion Laboratory of the California Institute of Technology for their continued support of his role in providing insight into the process of risk mitigation for conjunctions.

7. REFERENCES

1. Vincent, M.A. and Garcia, M.D., The Plans for Getting OCO-2 into Orbit., Proc. of AAS/AIAA Astrodynamics Specialist Conference, Girdwood, Alaska July 31-August 4, 2011.
2 Vincent, M.A. How to Enter, Fly In, and Exit the A-Train Constellation, Proc. Of the 8th International Workshop on Satellite Constellations and Formation Flying, Delft, The Netherlands, June 8-10, 2015.
3 "August 2014 CARA Users Forum: Updates to Concept of Operations," August 27, 2014
4 Private communication with B. Braun, analysis done by G. Peterson, October 4, 2012
5 Carpenter, J.R., Markley, F.L. and Gold, D., Wald Sequential Probability Ratio Test for Analysis of Orbital Conjunction Data, AIAA Guidance, Navigation, and Control (GNC) Conference, 2013.
6 Newman, L.K., Frigm, R.C., Duncan, M.G. and Hejduk, M.D., Evolution and Implementation of the NASA Robotic Conjunction Assessment Risk Analysis Concept of Operations, AMOS, 2014
7 Alfano, S, Relating Position Uncertainty to Maximum Conjunction Probability, J. Astronautical Sci, Vol. 53, No.2, 2005.
8 Scheeres, D.J., Hsiao, F.Y-., Park, R.S., Villac, B.F. and Maruskin, J.M., Fundamental Limits on Spacecraft Orbit Uncertainty and Distribution Propagation, J. of the Astronautical Sciences, Vol. 59, , Dec. 2006.
9 Scheeres, D.J., de Gosson, M.A. and Maruskin, J.M. Application of Symplectic Topology to Orbit Uncertainty and Spacecraft Navigation, J. of the Astronautical Sciences, Vol. 59, Jan-June, 2012.

10 Uhlmann, J., Dynamic Map Building and Localization: New Theoretical Foundations (Ph.D. thesis). University of Oxford, 1995.
11 DeMars, K.J., Bishop, R.H. and Jah, M.K., Entropy-Based Approach for Uncertainty Propagation of Nonlinear Dynamical Systems, J. of Guidance, Control, and Dynamics, Vol. 36, No. 4, July–August 2013
12 Norgaard, M., Poulsen, N.K. and Ravn, O., New developments in state estimation for nonlinear systems, Automatica, Vol. 36, Issue 11, pp. 1627-1638, Nov. 2000.
13 Jones, B.A., Doostan, A. and Born, G.H., Nonlinear Propagation of Orbit Uncertainty Using Non-Intrusive Polynomial Chaos, J. of Guidance, Control, and Dynamics, Vol. 36, No. 2, March–April 2013
14 Vittaldev, V. and Russell, R.P., Collision Probability for Space Objects using Gaussian Mixture Models." Advances in the Astronautical Sciences. Vol 148, AAS 13-351, 2013.
15 Ambadan, J.T. and Tang, Y., Sigma-Point Kalman Filter Data Assimilation Methods for Strongly Nonlinear Systems, J. Amos. Sci., Vol. 66, Issue 2, Feb. 2009.
16 Tapley, B.D., Schutz, B.E. and Born, G.H., Statistical Orbit Determination, Elsevier Academic Press, 2004
17 Stauch, J. and Jah, M.K., Unscented Schmidt-Kalman Filter Algorithm, J. of Guidance, Control, and Dynamics, Vol. 38, No. 1, Jan. 2015
18 Heyduk, M.D., Response to Action Item from the Earth Science Constellation Mission Operations Working Group (MOWG) meeting: ASW Covariance Improvements and JMS Delivery Strategy/Schedule, email sent Aug. 26, 2015
19 Duncan, M.G. and Long, A., Realistic Covariance Prediction for the Earth Science Constellation, Proc of the AIAA/AAS Astrodynamics Specialist Conference; Keystone, CO, Aug. 21-23, 2006
20 Heyduk, M.D., Covariance Realism Evaluation Approaches, GSFC FDSS-II Task Order 16 Technical Memorandum, July 10, 2015
21 Lechtenberg, T., Wysack, J., Hasan, S.O. and Guit W.J., Realistic Covariance Generation in the Presence of Maneuvers, Proc. of AIAA/AAS Astrodynamics Specialist Conference, Vail, Colorado, Aug. 10-13, 2015
22 Frigm, R.C., Total Probability of Collision as a Metric for Finite Conjunction Assessment and Collision Risk Management, Proc. of the Advanced Maui Optical and Space Surveillance Technologies Conference, Wailea, Maui, Hawaii, September 16-18, 2015.
23 Alfano, S., Review of Conjunction Probability Methods for Short-Term Encounters," Proc. of AAS/AIAA Space Flight Mechanics Meeting, Sedona, AZ, in, Advances in the Astronautical Sciences Series 127, 2007.
24 Chan, K., Spacecraft Collision Probability for Long-Term Encounters, Proc. of AAS/AIAA Astrodynamics Specialist Conference, Big Sky, Montana, Aug. 3-7, 2003.
25 McKinley, D.P., Development of a Nonlinear Probability of Collision Tool for the Earth Observing System, AAS/AIAA Astrodynamics Specialist Conference, Keystone, Colorado, Aug 21-24, 2006.
26 Duncan, M.D. Wysack, J. and Frisbee J., Collision Probability Forecasting using a Monte Carlo Simulation, Proc. of the Advanced Maui Optical and Space Surveillance Technologies Conference, Wailea, Maui, Hawaii, September 9-12, 2014.
27 Cerven, W.T., Bounding Collision Probability Updates, Proc. Of AIAA/AAS Astrodynamics Specialist Conference, Vail, Colorado, Aug. 10-13, 2015.
28 Vallejo J., and Hejduk, M.D., Proc. of AIAA/AAS Astrodynamics Specialist Conference, Vail, Colorado, Aug. 10-13, 2015.